RSC Sustainability

ROYAL SOCIETY OF CHEMISTRY

PAPER

View Article Online
View Journal | View Issue

Cite this: *RSC Sustainability*, 2024, **2**, 2312

Sustainable dissolution of collagen and the formation of polypeptides in deep eutectic solvents for application as antibacterial agents†

Harmandeep Kaur,[a] Manpreet Singh,[a] Navdeep Kaur,[b] Pratap Kumar Pati,[b] Monika Rani[c] and Tejwant Singh Kang *[a]

Collagen is a protein that is hard to dissolve in water and many other solvents, which limits its applications. Herein, deep eutectic solvents (DESs), *i.e.* choline chloride : lactic acid (ChCl : LA) = 1 : 1 and ethylene glycol : zinc chloride (EG : $ZnCl_2$) = 4 : 1, are effectively used to dissolve type I collagen under different conditions. Type I collagen is readily soluble at a concentration of 9.5–22.5 w/v% in DESs, and the solubility is governed by the nature of the DES, temperature (45 °C, 70 °C and 90 °C) and the absence or presence of $HCl_{(aq.)}$ (5×10^{-5} M). The dissolved material is regenerated by employing ethanol as an anti-solvent at 4 °C and investigated for alteration in the polymeric structure using Fourier-transform infrared spectroscopy (FTIR), circular dichroism (CD), UV-vis spectroscopy, X-ray diffraction (XRD), thermogravimetric analysis (TGA), and SDS-PAGE techniques. The increase in temperature and the presence of dilute $HCl_{(aq.)}$ result in a relatively greater disruption of the H-bonded structure of collagen, causing the unwinding of its triple-helical structure coupled with reduction in the helical content of polyproline type-II helices, which exposed vital amino acid residues in the regenerated material. Such an unwinding is accompanied by the formation of low molecular weight polypeptides, which are readily soluble in water and show antimicrobial activity comparable to or more than that exhibited by a model antibiotic Kanamycin towards both Gram-negative and Gram-positive bacteria. DESs are reused for at least 3 cycles for collagen solubilization without alteration in their inherent structure and collagen solubilizing ability, whereas the material regenerated from reused DESs shows properties similar to that shown by the material regenerated from virgin DESs. In this manner, a new sustainable strategy for solubilizing collagen and the direct preparation of essential and active low molecular weight collagen peptides directly from collagen in a single step is established. An inventive approach to using collagen is made possible by the observation that lower molecular weight peptides formed from the sustainable dissolution of collagen with exposed aromatic amino acid residues can demonstrate antibacterial activity.

Received 11th March 2024
Accepted 18th June 2024

DOI: 10.1039/d4su00122b

rsc.li/rscsus

Sustainable spotlight

Collagen is one of the most important and abundant proteins in mammals, and has many important applications. The presence of H, ionic, and hydrophobic bonds as well as electrostatic interactions makes the triple-helical structure of collagen stable; therefore, collagen is considered a hard-to-dissolve polymer that limits its applications. Collagen can otherwise be dissolved in organic solvents or highly acidic media, which is not an environment-friendly option. Therefore, new environment-friendly and cheaper solvents should be used to dissolve collagen and transform it into value-added materials. Herein, the solvents used for the dissolution of collagen, *i.e.* deep eutectic solvents (DESs), are green, cost-effective, biodegradable, easy to prepare, and environment-friendly compared to other conventional solvents. The material regenerated from DESs after the dissolution of collagen at a relatively lower temperature (45 °C) shows properties similar to native collagen. Moreover, the material regenerated from DESs after the dissolution of collagen at 70 °C and 90 °C exhibits properties akin to gelatin and smaller molecular weight polypeptides. The obtained polypeptides exhibited enhanced antimicrobial activity against both Gram-positive and Gram-negative bacteria, which was even higher than Kanamycin (standard antibiotic). With further research, such materials may be used as biological antimicrobial agents. Further, no harmful organic solvent was used during the synthesis of DESs and thus does not pose any risk to the environment. DESs are recycled and reused, adding to the sustainability of the process. Considering the above premises, the present work certainly emphasizes the following UN sustainable development goals: good health and well-being (SDG3); affordable and clean energy (SDG7); industry, innovation, and infrastructure (SDG9); responsible consumption and production (SDG12), and establish and organize climate action (SDG13).

[a]*Department of Chemistry, UGC Centre for Advanced Studies-II, Guru Nanak Dev University, Amritsar-143005, India. E-mail: tejwantsinghkang@gmail.com; Tel: +91-183-2258802-Ext-3291*

[b]*Department of Biotechnology, Guru Nanak Dev University, Amritsar-143005, India*

[c]*Department of Food Science and Technology, Guru Nanak Dev University, Amritsar-143005, India*

† Electronic supplementary information (ESI) available. See DOI: https://doi.org/10.1039/d4su00122b

1 Introduction

Collagen is one of the most vital proteins in mammals, corresponds to three-quarters of the dry weight of the human skin, and is a widespread component of the extracellular matrix.[1–3] Among the various types of collagen,[2] type I collagen has gained much attention owing to its wide application. Structurally, type I collagen is a cylindrical entity exhibiting a right-handed triple-helical structure comprising three polyproline type-II helices, which wind around each other to form a rod-like right-handed super helix[2] with a molecular weight of ~300 kDa,[4,5] length of ~280 nm and diameter of ~1.4 nm.[5,6] The three helically twisted polypeptide alpha chains[5–7] have repeated units of amino acids, such as Gly-X–Y, where X and Y are proline and 4-hydroxy proline, respectively.[1,3,5] Glycine is buried inside the core of the triple-helical structure, and X and Y residues are exposed to the solvent.[8,9] The regions at the end of the N- and C-terminus that do not form a triple helical structure are called telopeptides.[8,9] Telopeptides typically consist of 15–26 amino acid residues, such as lysine and hydroxylysine, along with their aldehyde derivatives, and are crucial for the creation of both intramolecular and intermolecular covalent crosslinks.

Type I collagen exhibits low antigenic and high direct cell adhesion properties and has been extensively used as a biomaterial for the development of tissue engineering constructs and wound dressing systems.[9,10] Partial hydrolysis of collagen yields gelatin,[11–13] a valuable water-soluble protein that has received considerable attention due to its mineral binding capacity, lipid-lowering effect, immunomodulatory[13] and antihypertensive response along with antioxidant[13,14] and antimicrobial properties,[13] and other applications that are associated with the presence of low molecular weight peptides. The various applications of collagen and its hydrolysed product, gelatin, have made collagen an interesting material to be explored further. Type I collagen is soluble in inorganic (sodium hypochlorite)[15] and acts as organic solvents/acids[16] but at a relatively higher temperature. The toxic nature of such solvents and the high-temperature conditions of solubilization renders the solubilization non-sustainable and limits the applications of collagen. However, it is non-soluble in water owing to its ordered structure supported by inter- and intra-molecular H-bonds,[17] hydrophobic interactions, ionic interactions and van der Waal's forces.[18,19] Therefore, new sustainable methods of dissolution, modification or preparation/extraction of collagen peptides/collagen hydrosylates, and subsequent regeneration need to be devised to widen the application of collagen. A detailed comparison of the method in this study with previously reported methods for dissolving collagen and preparing collagen peptides is provided in Annexure S1 (ESI),† revealing that the present method considers all the goals of "Green chemistry".

To advance in this area, ionic liquids (ILs), which comprise only ions[20–22] and are accepted as relatively greener solvents, have been tested as media for solubilizing collagen[23,24] considering their ability to dissolve many hard-to-dissolve materials.[25,26] The solutions of imidazolium-based ILs in acetate buffer have been found to exert stabilizing or destabilizing effects on the helical structure of type I collagen governed by the nature of ions comprising ILs.[24] The lyophilized collagen (type I from calf skin) has also been reported to be soluble in concentrated aqueous solutions of imidazolium-based ILs, $[C_2mim][BF_4]$ and $[C_2mim][Ac]$; however, the maximum yield of dissolution was quite low (3.57 mg ml^{-1}).[27] There are few examples of ILs that can dissolve collagen except for 1-butyl-3-methylimidazolium chloride, $[C_4mim][Cl]$, which was found to dissolve collagen in good yield by Meng *et al.*[19] The high chloride concentration is effectual in breaking the H-bonds and the ionic bonds in the collagen and thus leads to its dissolution similar to that observed in the case of dissolution of wood,[28] cork,[29] cellulose,[25] wool keratin,[30] and silk fibre[31] in ILs. Therefore, few advancements in the dissolution of collagen utilizing ILs have been reported. More importantly, the triple helical structure of native collagen and the effectiveness of essential amino acids are noticeably destroyed during the dissolution processes.

The quest to develop new benign solvents has led to another class of widely accepted green solvents called Deep Eutectic Solvents (DESs). DESs are the eutectic mixtures of two or three molecular components (ionic or uncharged), H-bond donor (HBD), and H-bond acceptor (HBA), and they have melting points far below that of the individual components.[32–34] The lowering of melting point is ascribed to the charge delocalisation *via* H-bond interactions of complexing agent (typically H-bond donor) with the halide anion, which in turn reduces the anion's interaction with its parent cation results in the formation of complex anionic species.[35] DESs exhibit properties akin to ILs such as low volatility, recyclability, non-flammability, and excellent thermal stability[32,36] but are biocompatible, easy to prepare without the use of any organic solvent in a single-step reaction, and cost-effective. This, along with the possibility of offering multiple H-bonding interactions by DESs to polymers/biopolymers,[37,38] renders DESs as green solvents of choice for the dissolution and simultaneous preparation of collagen peptides from collagen under optimal conditions. A range of processing methods have been applied to produce collagen peptides or hydrolyzed collagen. However, the collagen structure is severely degraded to the molecular level during the dissolution/extraction processes, leading to a weakened performance of the obtained collagen-based materials with a low yield. What basically hinders the direct extraction of active collagen peptides is the complicated hierarchical structure, non-collagenous proteins and nucleic acid present along with the raw material. This gap drives us to directly obtain lower molecular weight collagen peptides with exposed active amino acids from natural collagen to reserve nanostructures. Although the extraction of collagen peptides from collagen has been reported in DESs,[39,40] to the best of our knowledge, there is no report concerned with thorough investigations on the use of DESs for the dissolution and regeneration of collagen along with the formation of gelatin/collagen peptide to be used as antimicrobial agents.

Herein, DESs comprising (i) choline chloride (ChCl) and LA (ChCl : LA = 1 : 1) and (ii) ethylene glycol (EG) and $ZnCl_2$ (EG : $ZnCl_2$ = 4 : 1) have been successfully established as dissolution

media for type I collagen. The choice of the components of DESs is because the presence of Cl^- and OH-along with the Lewis acidity of $ZnCl_2$ has been found to aid in the dissolution of hard-to-dissolve polymers, such as cellulose,[25] keratin,[37,41] PET,[42,43] polythene[44] and wheat straw,[45] when present as one of the components in ILs[25] or DESs.[37,41–45] LA-based DESs have also been used as a solvent for the exfoliation of biopolymers.[46,47] $ZnCl_2$ as Lewis acid is expected to activate the –C═O group of amino acids and –OH groups of EG in the presence of light. Further, Cl^- of $ZnCl_2$ could form H-bonds with collagen and is thus supposed to break the amide bonds in collagen. In the case of ChCl : LA, the –OH and –C═O groups of LA and Cl^- of ChCl undergo the H-bonding interactions required to dissolve and degrade collagen.

Various conditions of temperature (45 °C, 70 °C and 90 °C) and the presence of 5×10^{-5} M of dilute $HCl_{(aq.)}$ have been tested for the dissolution and processing of collagen in DESs. A temperature increase is expected to enhance the solubilization of collagen in DESs. Besides, the presence of 5×10^{-5} M concentration of $HCl_{(aq.)}$ in DESs could result in the protonation of the $–NH_2$ group of amino acid residues of collagen, which favour the dissolution of collagen by offering electrostatic repulsion between similarly charged groups. Collagen dissolved in DESs is regenerated using ethanol as an antisolvent at 4 °C. The structure and properties of the regenerated material are explored and compared with those of native collagen using various state-of-the-art techniques. Based on the conditions, the regenerated material is found to be (i) collagen and (ii) low molecular weight collagen peptides. Regenerated collagen and collagen peptides are known to exhibit remarkable antimicrobial activity against Gram-positive and Gram-negative bacteria, which is almost or even better in some cases than that shown by the antibiotic Kanamycin. Compared to ILs and other processing techniques, DESs can disassemble the original triple helical structure and preserve the nanofibrous structure with active vital aromatic amino acids. In a way, a new sustainable method for the dissolution of hard-to-dissolve biopolymer, collagen, in DESs and its transformation to low molecular weight peptides in a single step, which exhibits remarkable antimicrobial activity, is established. The current work is anticipated to offer a new platform not only for the sustainable dissolution and preparation of collagen peptides from collagen but also for the dissolution and processing of many other biologically important polymers for diverse applications.

2 Experimental section

2.1. Materials

Collagen from bovine achilles tendon (type I) was purchased from Sigma-Aldrich. Ethylene glycol (EG) (>98%) and lactic acid (LA) (>88%) were purchased from Loba Chemie, India. Zinc chloride ($ZnCl_2$) (>98%) was bought from Spectrochem Pvt Ltd, Mumbai, India, and choline chloride (ChCl) (>98%) was purchased from Sigma-Aldrich. Ethanol (AR grade) was procured from SD Fine Chemicals Ltd, Mumbai, India. AR grade sodium acetate (>99%) and acetic acid (>99.7%) were used to prepare acetate buffer and were bought from SRL, India. A protein molecular weight marker, a broad range (25 lanes), and 0.25 ml of SKU PMWB1 were purchased from GeNei.

2.2. Dissolution and regeneration of collagen at different temperatures

Different Deep Eutectic Solvents (DESs), *i.e.* (i) ethylene glycol (EG) : zinc chloride ($ZnCl_2$) in molar ratio 4 : 1 and (ii) choline chloride (ChCl) : lactic acid (LA) in molar ratio 1 : 1, were synthesized as reported earlier.[48,49] Thus, the obtained clear and homogenous DESs were stored in a desiccator to avoid the absorption of moisture. The solubility limit of collagen in DESs was first ascertained by adding collagen fibrils in lots (5 mg per lot) to 1 ml of respective DES preheated at 45 °C with continuous stirring at 100 rpm. The solubilization of collagen was monitored at different temperatures (45 °C, 70 °C and 90 °C) in the absence and presence of 5×10^{-5} M concentration of diluted $HCl_{(aq.)}$ using an optical microscope. 5 μL of 0.01 M $HCl_{(aq.)}$ (5×10^{-5} M) was added to 1 ml of the respective DES, which did not alter the pH noticeably of otherwise acidic DESs. The presence of collagen fibrils, even after stirring for a long time under specific conditions, marks the solubility limit of collagen in DESs. Later, for a regeneration process, ethanol (2 ml) was used as an antisolvent to 1 ml of the DES-collagen system at 4 °C. This resulted in the formation of white flocculent precipitations separated by centrifugation, followed by washing with ethanol 5 times. To ensure the complete removal of DESs, the FTIR of regenerated material is compared with native DESs (Fig. S1, ESI†).

2.3. Characterisation of native collagen and regenerated material

Fourier Transform-Infrared (FTIR) spectroscopy was used to study the chemical composition of native collagen and regenerated material using an Agilent Cary 630 spectrometer in the range of 400–4000 cm^{-1}. Circular dichroism (CD) spectroscopic measurements were performed by employing a BioLogic MOS-500 spectrometer in the wavelength range of 190–250 nm using a cuvette of path length 1 mm at a scan rate of 50 nm min^{-1}. A UV-vis spectrophotometer (Cary 5000 UV-vis-NIR) was used for UV-vis absorption measurements in the wavelength range of 400–800 nm using a quartz cuvette of unit path length. UV-vis and CD spectroscopic measurements were made by dissolving the respective material in acetate buffer (pH ~5.6). The crystallinity of native collagen and regenerated material was probed using X-ray diffraction (XRD) measurements employing a SHIMADZU MAXIMA ~70 000 instruments in the 2θ range of 5–80°. The thermal stability of the material was monitored using a HITACHI STA7200 thermal analyzer under an N_2 atmosphere at temperatures ranging from 25 to 1000 °C at a heating rate of 10 °C min^{-1}. The molecular weight of the native collagen and regenerated material (collagen and collagen peptides) was determined using SDS-Page (Mini-Protean Tetra Cell, Bio-Rad Laboratories, Hercules, USA) at a constant current of 25 mA in 8% resolving gel. Optical density was measured at 600 nm using a UV-visible true double-beam spectrometer (Motras Scientific).

2.4. Antibacterial activity assay

Antibacterial activity was evaluated against two Gram negative (*Escherichia coli* and *Pseudomonas syringae*) and two Gram positive (*Bacillus subtilis* and *Staphylococcus aureus*) bacterial strains. Antimicrobial activity assays were performed as per the method described by Ennaas *et al.* in 2016 with minor modifications.[50] All the samples with 1 mg ml^{-1} concentration of the material were serially diluted 2-fold in Luria Bertani (LB) broth. 100 μL of bacterial suspension (~1 × 10^6 CFU per ml) of the given bacterial strain was seeded into all the samples. The samples were incubated at 37 °C in the case of *E. coli* and *S. aureus*, 28 °C in the case of *P. syringae*, and 30 °C for *B. subtilis.* Kanamycin (1 mg ml^{-1}) was used as a reference. All the samples were incubated for 24 h with a given bacterial strain, and absorbance was measured at 600 nm. The data were statistically analysed using a one-way analysis of variance (ANOVA) (the Fischer LSD) (Sigma Stat version 3.5).

3 Results and discussion

3.1. Solubility of collagen in DESs

The synthesized DESs, *i.e.* (i) EG : $ZnCl_2$ (4 : 1) and ChCl : LA (1 : 1), are tested for dissolving collagen (type I) under different conditions. The extent of dissolution of collagen and the yield of the regenerated material in the investigated DESs under different conditions are illustrated in Table 1. Collagen dissolves in both the investigated DESs in appreciable amounts, where the solubility of collagen is found to be in the range of 9.5–22.5 w/v%. At any temperature, in the absence and presence of $HCl_{(aq.)}$, EG : $ZnCl_2$ shows a higher solubilizing ability towards collagen compared to ChCl : LA. An increase in temperature results in an increase in the solubility of collagen in both DESs. However, the increase is more pronounced in the case of EG : $ZnCl_2$ (~2.2 mg ml^{-1} °C^{-1}) compared to that observed in ChCl : LA (~1.2 mg ml^{-1} °C^{-1}) (Fig. S2, ESI†). The presence of $HCl_{(aq.)}$ in the investigated DESs at any of the investigated temperatures enhances the solubility of collagen (Table 1). To have a broader idea about the change in the molecular structure of collagen upon dissolution, followed by regeneration, the solubility of the regenerated material was checked in water at room temperature. Interestingly, some parts of the regenerated material obtained from the dissolution of collagen at 70 °C in the presence of $HCl_{(aq.)}$ in both of the DESs are found to be soluble in water, whereas the entire regenerated material obtained after the dissolution of collagen at 90 °C in the presence and absence of $HCl_{(aq.)}$ is dissolved in water. The details about the role of DESs, temperature and acidic conditions in the dissolution of collagen and modification in the structural arrangement of collagen along with the formation of water-soluble material under certain conditions are thoroughly discussed in the later sections of this paper.

3.2. Structural characterization of regenerated material

The collagen is dissolved in different DESs under different conditions of temperature in the presence and absence of $HCl_{(aq.)}$. Therefore, for better understanding, the regenerated material is abbreviated in accordance with the condition as R1-(*T*), R2-(*T*) and R1-(*T*)-A and R2-(*T*)-A, where R represents regenerated material; 1 and 2 denote ChCl : LA (1 : 1) and EG : $ZnCl_2$ (4 : 1), respectively; *T* is the temperature of dissolution; and A corresponds to acidic conditions (in the presence of $HCl_{(aq.)}$).

3.2.1. Fourier-transform infrared (FTIR) spectroscopy. Fig. 1A depicts the FTIR spectra of R1-(45) and R2-(45) in comparison to native collagen. FTIR spectra of collagen as well as of R1-(45) and R2-(45) show the characteristic bands at 3287 cm^{-1} and 2958 cm^{-1}, which are assigned to N–$H_{(str.)}$ of the H-bonded N–H groups of the amide-A and amide-B bands, respectively.[49] R1-(45) shows negligible change in the band position, whereas R2-(45) exhibits a blue shift (~3302 cm^{-1}) in the band position of the amide-A band compared to that shown by collagen (3287 cm^{-1}). The results suggest a relatively more disruption of the H-bonding network of collagen in the case of R2-(45). The formation of relatively weak H-bonding between free hydroxyl groups (–OH) of EG of DES and amino groups of amino acid residues of collagen at the cost of partial disruption of inter- and intra-molecular H-bonds within collagen during dissolution could lead to such a blue shift. The changes in the triple-helical structure of collagen during dissolution can also be probed by alterations in the position as well as the intensity of amide-I, amide-II and amide-III bands.[51,52] The band at 1600–1660 cm^{-1} (amide-I) corresponds to the stretching vibration of amide carbonyls along the polypeptide backbone of native collagen, while the band around 1550 cm^{-1} (amide-II) in native collagen is associated with N–$H_{(bending)}$ and C–$N_{(str.)}$ vibrations.[53,54] Three bands around 1200–1237 cm^{-1} are termed amide-III bands and assigned to C–$N_{(bending)}$ and N–$H_{(bending)}$ vibrations as well as wagging vibrations of –CH_2 groups of side

Table 1 Solubility of collagen and yield of the regenerated material in DESs at different temperatures in the presence and absence of $HCl_{(aq.)}$

	45 °C			70 °C			90 °C		
DESs	Time (h)	Solubility (mg ml^{-1})	Yield (mg)	Time (h)	Solubility (mg ml^{-1})	Yield (mg)	Time (h)	Solubility (mg ml^{-1})	Yield (mg)
ChCl : LA	4.0	95	55	3.0	120	90	2.0	150	100
EG : $ZnCl_2$	2.5	110	70	2.0	185	160	1.0	210	170
ChCl : LA + $HCl_{(aq.)}$	3.0	120	90	2.0	130	95	1.0	195	157
EG : $ZnCl_2$ + $HCl_{(aq.)}$	2.0	166	145	1.0	170	155	0.5	225	195

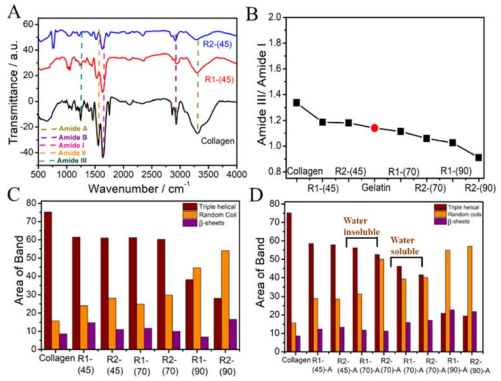

Fig. 1 (A) FTIR spectra of native collagen and the material regenerated from the dissolution of collagen from ChCl : LA and EG : $ZnCl_2$; (B) amide III/amide I ratio of native collagen, gelatin and the material regenerated from DESs under different temperature conditions; and (C and D) band area of amide-I band of collagen and the material regenerated from DESs under different conditions.

chains of proline residues and the backbone of glycine molecules. Both the amide-I and amide-II bands undergo a red shift compared to collagen in the cases of R1-(45) and R2-(45), suggesting a weakening of the H-bonding network of collagen. A decrease in the band intensity of the amide-I and amide-II bands in the order collagen >R1-(45) > R2-(45) suggests a reduced number of H-bonds, which stabilizes the triple-helical structure of collagen. Further, the ratio of intensities of the amide-III to amide-I band can be used to elucidate the loss or gain of secondary structure (2°-structure) in terms of alterations in the content of random coil/α-helix or triple helix, respectively.[55] A marginal decrease in the ratio of intensities of amide-III to amide-I bands (Fig. 1B) in R1-(45) and R2-(45) suggests a partial decrease in the triple-helical content of collagen.

It is deduced that although collagen mainly preserves its structure, some disorders occur in the triple-helical structure of collagen. With an increase in dissolution temperature, the amide-A band (3287 cm^{-1}) is broadened, where the broadening follows the order R1-(45) < R1-(70) < R1-(90) and is more in the case of R2 compared to R1 at all of the investigated temperatures (Fig. S3, ESI†). This suggests an increasing extent of disruption of the H-bonding network of collagen at higher temperatures, which is more in the case of R2 compared to R1. The ratio of the amide-III to amide-I band decreases as temperature increases (Fig. 1B) following the order R1-(45) < R1-(70) < R1-(90), which falls even below that shown by gelatin, a linear polypeptide and hydrolysis product of collagen in the case of R1-(90) and R2-(90).

This indicates the complete loss of 2°-structure and unfolding of collagen at higher temperatures, leading to the formation of random coils and other structures. The heterogeneity in the carbonyl groups and their coupling in stretching modes results in complexity in the amide-I region; thus, it is important to focus on this area to understand the different structural components of collagen. Therefore, deconvolution of the amide-I region is performed to compare the 2°-structure of native collagen and regenerated materials.[55] The different structural components in native collagen, such as β-sheets, random coils and triple-helical structures, are centred around 1612 cm^{-1}, 1630 cm^{-1} and 1664 cm^{-1}, respectively, in the amide-I band.[55] The change in band area and position in regenerated material represents the changes in the relative content of 2° structural components under different conditions (Fig. 1C and Table S1, ESI†). In comparison with collagen, R1-(45) shows a ~15% increase in the content of random coils at the cost of a decrease in the content of β-sheets to a similar extent, which is relatively more in the case of R2-(45), where the content of triple-helical structures remains approximately the same. Relatively more loss in the content of β-sheets is observed in the case of R1-(70) and R2-(70). However, a drastic decrease in the content of the triple-helical structure of collagen from 75% to 40% and 27%, and an increase in the content of random coils from 15% in collagen to 45% and 55% in the case of R1-(90) and R2-(90), respectively, suggests complete disruption of the triple-helical structure of collagen at elevated temperatures. The observance of low molecular weight peptides along with the partially unfolded collagen in the case of R1-(70) and R2-(70) and the peptides only at R1-(90) and R2-(90) supports the above inference (discussed later). At different temperatures, the impact of $HCl_{(aq.)}$ in DESs on the properties of regenerated material is also investigated. No significant change in the characteristic properties of R1-(45)-A and R2-(45)-A is observed, as inferred from FTIR investigations (Fig. S4A, ESI†). Moreover, R1-(70)-A and R2-(70)-A are found to be partially soluble in water, whereas R1-(90)-A and R2-(90)-A are completely soluble in water similar to that observed in the case of R1-(90) and R2-(90).

FTIR spectra of water-insoluble material (from R1-(70)-A and R2-(70)-A) (Fig. S4B, ESI†) resemble those of collagen (Fig. S3A, ESI†). Furthermore, water-soluble material from R1-(70)-A and R2-(70)-A (Fig. S4B, ESI†) and (R1-(90)-A and R2-(90)-A) (Fig. S4C, ESI†), expected to be low molecular weight peptides, exhibits a relatively broadened amide-A band (3290 cm^{-1}), red-shifted amide-III (1650 cm^{-1}) and amide II (1550 cm^{-1}) bands mimicking the bands shown by gelatin (Fig. S3B, ESI†). This suggests the formation of water-soluble polypeptides structurally similar to that of gelatin devoid of any 2°-structure, where the complete loss of triple-helical content is supported by the absence of three bands in the amide-III region (1200–1237 cm^{-1}). No significant difference in the 2°-structural components between R1-(45) and R1-(45)-A is observed from the deconvolution of the amide-I band (Fig. 1D). R1-(70)-A exhibits marginal loss in the triple-helical content at the cost of a similar increase in the content of random coils compared to R1-(70), whereas a significant increase in the content of random coils and loss in the triple-helical structure is observed in the case of R2-(70)-A compared to R2-(70) (Fig. 1D). The presence of $HCl_{(aq.)}$ results in the unwinding of the triple-helical structure of collagen, the effect of which is more at higher temperatures, as suggested by relative values of amide III/amide I ratio (Fig. S4D, ESI†), which is in line with the observations made from deconvolution of the amide-I band (Fig. 1D).

3.2.2. Circular dichroism spectroscopy. A comparison of the Circular Dichroism (CD) spectra of the regenerated material

with that of collagen is made to support the inferences made from FTIR-spectroscopy in terms of the alterations in the 2°-structure of collagen during dissolution (Fig. 2). The characteristic line shape in the CD spectra of collagen signifies the highly ordered conformations of the amide bonds of various amino acids in the α-helices. CD spectra of collagen exhibit a prominent negative band in the range of 200–215 nm (Fig. 2), which corresponds to amide transitions in a triple-helix conformation.[56] A positive band ranging from 215 to 230 nm centred around 220 nm is attributed to the "polyproline-II" helical content. A decrease in the ellipticity accompanied by a red shift of the negative band in the case of R1-(45) and R2-(45) (Fig. 2A and B) indicates partial unfolding of triple-helical confirmations, leading to exposure of amine groups towards solvent. Such an unfolding obviously accompanies the disruption of H-bonding interactions between polypeptide chains as suggested by FTIR-spectroscopy. Additionally, a marginal decrease in ellipticity along with a negligible change in the line shape of the positive band suggests non-significant alterations in the "polyproline-II" helices.

The ellipticity of the positive band decreases with an increase in the temperature of dissolution, which almost disappears in the case of R1-(90) and R2-(90) without any discrimination towards DES used (Fig. 2A and B). This indicates the complete disruption of the "polyproline-II" helical structure *via* the breakage of H-bonds between proline/hydroxy-proline amino acid residues.

A single negative band peculiar to the triple-helical structure in collagen transforms into two narrowly separated bands located at ~205 and ~210 nm in the case of R1-(70) and R2-(70), respectively, which further shifts red accompanied by a decrease in ellipticity in the case of R1-(90) and R2-(90) (Fig. 2A and B). The band at ~205 nm closely resembles that shown by polyproline-II[56] with a helical structure, the content of which decreases with an increase in temperature as also suggested by the disappearance of the positive band ~222 nm at higher temperatures. The appearance of the band around 210 nm, which shifts red at higher temperatures, is assigned to the formation of the β-sheet structure, which may be present in the random coils.[57] Further, a red shift suggests the breaking of peptide bonds, which could result in the formation of low molecular weight polypeptides with a structure similar to random coils or unordered peptides. Many unordered polypeptides with different compositions stabilized *via* hydration show such features in the CD spectra.[57,58] The presence of $HCl_{(aq.)}$ does not affect the line shape of both CD bands in the case of R1-(45)-A and R2-(45)-A to an appreciable extent compared to that of collagen (Fig. 2C and D) in line with the observations made from FTIR-spectroscopy. Water insoluble R1-(70)-A retains the shape of a negative CD band, and it shifts towards red, whereas a change is observed in the shape of the CD band in the case of water-insoluble R2-(70)-A, water-soluble R1-(70)-A and R2-(70)-A. This along with the complete loss of a positive CD band in the case of water-soluble and water-insoluble R1-(70)-A and R2-(70)-A (Fig. 2C and D) suggests that the triple-helical structure of collagen is appreciably unfolded at higher dissolution temperatures in the presence of $HCl_{(aq.)}$, resulting in its partial transformation to water soluble low molecular weight polypeptides displaying no characteristic band of "polyproline-II" type helices. The appearance of a symmetric negative band at 215 nm and the complete loss of a positive band at 222 nm specific to the "polyproline-II" helical structure in the case of R1-(90)-A and R2-(90)-A (Fig. 2C and D) reveals the complete disruption of the triple-helical structure of collagen and the formation of β-sheets and random coils. On comparing, it is observed that although there is disruption of the H-bonded network of amino-acid residues in both the "polyproline-II" helices and triple-helical structure in the absence of $HCl_{(aq.)}$. However, the presence of $HCl_{(aq.)}$ completely transforms the collagen into polypeptides with random coils and β-sheet structure.

3.2.3. UV-vis spectroscopic investigations. UV-vis absorbance spectrum of native collagen exhibits a strong, π–π* type absorption band centred around 215 nm.[58] This absorption band arises from the electronic excitation of the π-system of keto, carboxylic acid and amide chromophores and thus reflects the framework conformation of protein. Another broad band in the range 240–300 nm is assigned to the presence of phenylalanine, tyrosine and tryptophan residues absorbing in the 250–270 nm, 270–290 nm and 280–300 nm regions, respectively.[8,59] The band corresponding to the peptide chain framework of native collagen at 215 nm is red shifted in the case of R1-(45) and R2-(45) to 230 and 240 nm, respectively (Fig. 3A and B); the partial hydrolysis of collagen during dissolution, the extent of

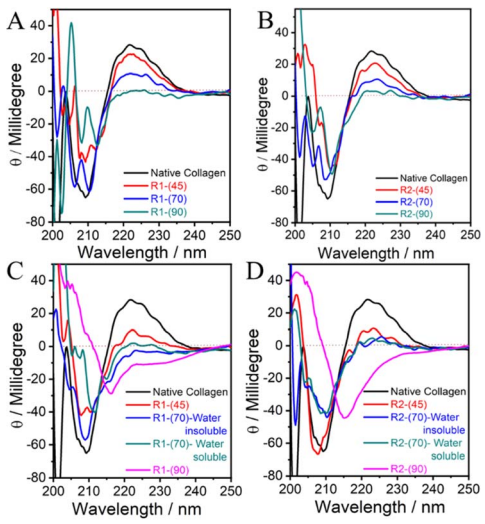

Fig. 2 (A–D) CD spectra of native collagen and the material regenerated from collagen dissolved in DESs under different conditions.

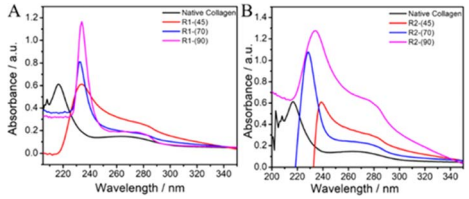

Fig. 3 UV-vis spectra of native collagen and the material regenerated after dissolution of collagen in (A) ChCl : LA and (B) EG : $ZnCl_2$ at different temperatures.

which seems to be more in the case of R2-(45), results in such a red shift.[60,61]

Generally, the hydrolysis of collagen occurs *via* the breakdown of amide bonds in polypeptide chains, which results in the appearance of free $-NH_2$ groups on the side chains of peptides, leading to a red shift in the absorption spectra. Similarly, the retention of the absorption bands in the range 240–300 nm suggests no alteration in the molecular structure of aromatic amino acid residues, whereas a red shift indicates the change in the molecular environment of these amino acid residues in regenerated material caused by disruption of the H-bonded network of collagen.

An increase in temperature results in red shift from ~215 nm to 230 and 240 nm in the material regenerated from ChCl : LA and EG : $ZnCl_2$, respectively. Besides, an increase in hyperchromicity of the bands (~215 nm and ~280 nm) with an increase in temperature for both of the investigated DESs is observed. This depicts the formation of random coil structure and exposure of free $-NH_2$ groups along with unmasking of aromatic amino acid residues (phenylalanine, tyrosine and tryptophan) upon hydrolysis, the extent of which is more in the case of R2 compared to R1.[62] This observation is in line with the results obtained from FTIR studies. Further, the absorption band observed at ~230 nm in the case of material regenerated in the presence of $HCl_{(aq.)}$ after dissolution at 70 °C and 90 °C resembles well the absorbance spectra of gelatin and peptides owing to prominent π–π* transitions (Fig. S5, ESI†). From the observations made from FTIR spectroscopy, CD spectroscopy and UV-vis absorption spectroscopy, it is inferred that there is a negligible effect of $HCl_{(aq.)}$ on the inherent structure and properties of material regenerated after dissolving collagen at 45 °C, whereas the presence of $HCl_{(aq.)}$ and high-temperature synergistically enhances the dissolution of collagen accompanied by the relatively greater unwinding of the triple-helical structure and "polyproline-II" helices, resulting in the formation of water-soluble polypeptides.

3.2.4. X-ray diffraction and thermogravimetric investigations. The alterations in the ordered arrangement of helices in collagen as a consequence of interactions with DESs during dissolution are monitored by X-ray diffraction (XRD) measurements (Fig. 4A). Native collagen shows a sharp diffraction peak centred around $2\theta = 7.5°$, which broadens in the case of R1-(45) and R2-(45)-A. This suggests an increase in the inter-chain distance,[53] caused by the weakening of the H-bonding network of collagen. The presence of a broader peak at $2\theta = 21.6°$ implies amorphous scatter resulting from unordered components of collagen, and another important but relatively weak scattering peak at $2\theta = 40°$ implies the prevalence of a typical triple-helical structure of collagen.[54] A decrease in the intensity of both of these peaks in the regenerated material suggests the partial unfolding of the triple-helical structure of collagen, which supports the inferences made from other techniques. The absence of a weak scattering peak at $2\theta = 7.5°$ in the XRD pattern of the R1-(70), R2-(70), R1-(90), and R2-(90) (Fig. S6A and B, ESI†) contrary to that observed at lower temperature supports the relatively greater unfolding of the triple-helical structure of collagen at higher temperature. XRD patterns could not resolve the structural differences for material regenerated in the presence of $HCl_{(aq.)}$ at all the investigated temperatures (Fig. S7, ESI†).

Thermogravimetric analysis (TGA) profiles of the native collagen and R1-(45) and R2-(45) (Fig. 4B) show the relatively lower thermal stability of regenerated material with degradation temperature, T_d ~230 °C, compared to native collagen with T_d ~250 °C. The presence of a relatively strong and greater number of H-bonds and ionic bonds in native collagen compared to those present in regenerated material offers higher thermal stability. The weight loss of native and regenerated collagen as a function of temperature is also examined. A small weight loss of ~100 °C represents the evaporation of physisorbed and bound water in native collagen and regenerated material (Fig. 4B). Another weight loss in the temperature ranging from 215 to 420 °C is ascribed to the degradation of side-chain groups of amino acids and thermal decomposition of polypeptide chains or higher molecular weight fractions.[63] At a temperature above 420 °C, another slight weight loss occurs in the case of native collagen and R1-(45). This loss ensues from the breakdown of the residual organic components such as derivatives of carboxy-terminal crosslinked telopeptides, helical peptides, or some residues with carbonaceous or nitrogenous content, which are the degradation products of collagen and are non-volatile.[64–66] A weight loss of ~20% in the temperature ranging from 420 °C to 600 °C in the case of R2-(45) is assigned to the decomposition of highly unordered polypeptide chains originated by the partial unfolding of triple-helical structure as suggested by FTIR results. Few changes in the thermal stability of the material regenerated at higher temperatures in the presence and absence of $HCl_{(aq.)}$ (Fig. S8 and S9, ESI†) are observed.

3.2.5. Molecular weight of regenerated material. The changes in molecular weight after regeneration from DESs are compared with native collagen using SDS-PAGE and their corresponding band positions, as shown in Fig. 5 and S10–S11 (ESI).† The detailed procedure for performing SDS-PAGE is provided in Annexure S2 (ESI).† The SDS-PAGE pattern of collagen type I comprises three main distinct bands: α-1 and α-2 monomer bands, and β- and γ-bands.[39,67] Amino acids, such as lysine and hydroxylysins, generally form inter- and intramolecular H-bonding between these chains. Additionally, histidine forms covalent crosslinking between the collagen molecules.[68,69] Bands of native collagen shown in Fig. 5, at apparent molecular weights of 129.4–110.0 kDa, 134.6–142.8 kDa and 191.9–198.7 kDa coincide with α-1, α-2 and β-band,

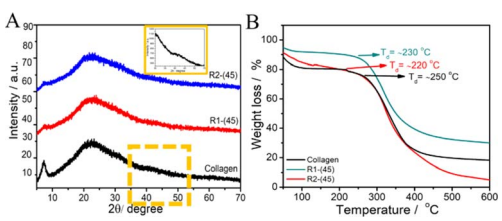

Fig. 4 (A) X-ray diffraction pattern and (B) TGA profiles of native collagen and the material regenerated from ChCl : LA and EG : $ZnCl_2$.

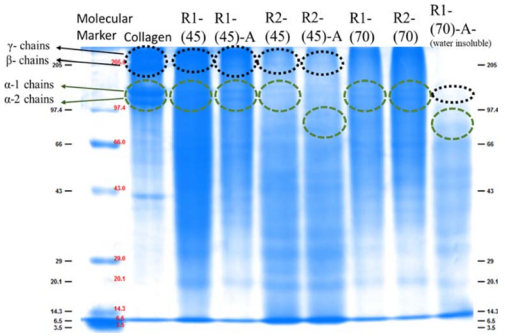

Fig. 5 SDS-PAGE displaying the molecular weight of the marker used, native collagen and the material regenerated after dissolution of collagen at 45 °C and 70 °C in ChCl : LA and EG : $ZnCl_2$.

respectively while γ-band is present at the top of the gel.[69] The β-band of collagen represents the dimeric form of α-1 and α-2 chains, or two α-1 chains and γ-band represent the trimeric form of three α-chains. These band patterns signify the folding of polypeptide chains in the triple-helical structure of native collagen. Interestingly, the bands corresponding to α-chains appear at a migrating distance similar to those of native collagen in all the regenerated materials attained from the collagen dissolved at 45 °C and 70 °C, as illustrated in Fig. 5. Nevertheless, their band intensity significantly decreases, suggesting the commencement of the unwinding of the triple-helical structure. In addition, a large number of electrophoretic bands (Fig. S9 and S10, ESI†) of different molecular weights presenting the fragmentation of collagen molecules during dissolution are observed (Table S2, ESI†).

However, in the case of the regenerated material obtained from collagen dissolved at 90 °C, band positions at lower molecular weight with weak intensity represent the intense fragmentation of collagen molecules with the complete disruption of the triple-helical structure both in the absence and presence of $HCl_{(aq.)}$, leading to the formation of polypeptides in both the employed DESs.

3.2.6. Mechanism of dissolution of collagen. Dissolution of collagen in DESs is governed by the disruption of inter- and intra-molecular H-bonds and ionic bonds between chains of collagen at the cost of attractive interactions between collagen and solvating DESs (Scheme 1). The presence of a large number of H- and O-atoms in various functional groups of different amino acid residues of collagen offers the sites for establishing H-bonding interactions with constituents of DESs as also observed in the case of extraction of collagen peptide by DESs.[39,40] In general, –OH, –C=O and $–NH_2$ groups of different amino acid residues of collagen interact with Cl^- of ChCl, –OH and –C=O groups of LA *via* H-bonding interactions in the case of ChCl : LA. Similarly, the –OH groups of EG and Cl^- of $ZnCl_2$ form H-bonds with collagen and thus break the amide bonds (Scheme 1) in the case of EG : $ZnCl_2$. Owing to its Lewis acidity, $ZnCl_2$ activates the –C=O group of amino acids, lowering the bond energy and thus making the bond easily breakable. Therefore, a relatively large number of –OH groups in EG and the presence of $ZnCl_2$ in EG : $ZnCl_2$ DES help in greater

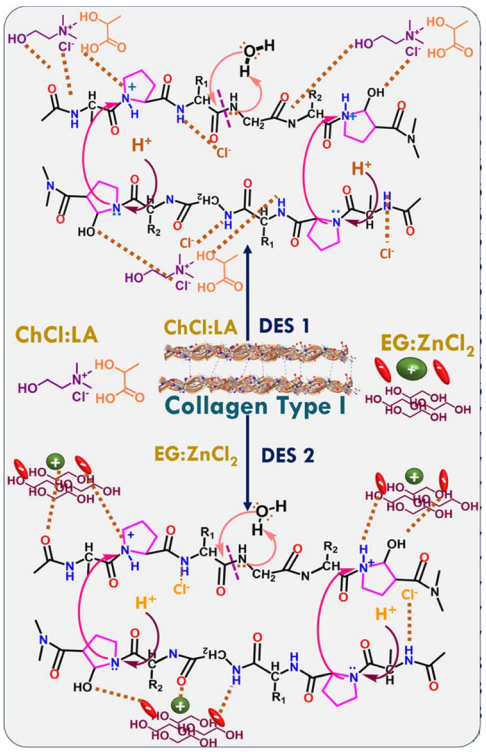

Scheme 1 Proposed mechanism of dissolution of collagen in DESs.

solubilization of collagen[44] at a faster rate compared to that observed in the case of ChCl : LA. The solubility of collagen increases as temperature increases, which is more pronounced at higher temperatures in both DESs (Table 1).

The thermal energy offered by high temperatures naturally lowers the activation energy of dissolution *via* the greater breakage of H-bonds between collagen fibrils. This results in the unfolding of a triple-helical structure as suggested by FTIR, CD and UV-vis absorption measurements and consequently offers more sites for components of DESs to engage in H-bonding with collagen in a synergistic manner and thus enhances the solubility. The solubility of collagen is also observed to increase under mild acidic conditions (Table 1). $HCl_{(aq.)}$ is expected to aid in the breaking of amide bonds in the polypeptides comprising collagen, leading to the appearance of low molecular weight polypeptides. Excess H^+ interacts with the imino of proline and hydroxyproline of collagen, resulting in the formation of ammonium salt, which further attracts more of Cl^- of DESs as well as of HCl, thus weakening inter- and intra-molecular H-bonding of collagen. An increase in temperature results in greater ionization of HCl in DESs; consequently, relatively more H^+ and Cl^- interacts with amino acid residues of collagen, leading to the breaking of H-bonds.[16] The protonation of the $–NH_2$ group of amino acid residues of collagen favours dissolution by offering electrostatic repulsion between similarly charged groups and facilitating the breakage of the H-bonding network in collagen at the cost of establishing H-bonding with Cl^- present in DESs. Comparing the effects of $HCl_{(aq.)}$ and temperature, it is observed that $HCl_{(aq.)}$ does not affect the extent of solubilization of collagen and properties of R1-(45)-A,

R2-(45)-A and R1-(70)-A, whereas the effect is more noticeable in the case of R2-(70)-A. Moreover, the structural alterations caused by collagen during dissolution are found to be comparable in the case of material regenerated at 90 °C in both DESs in the presence of $HCl_{(aq.)}$. To ascertain the formation of low molecular weight peptides, especially at higher temperatures and in the presence of $HCl_{(aq.)}$ as suggested by SDS-PAGE measurements, the solubility of the recovered material was examined. It is observed that the R1-(45), R2-(45), R1-(45)-A and R2-(45)-A are not water-soluble, whereas a part of the R1-(70)-A and R2-(70)-A is found to be water soluble. However, the material regenerated after dissolution at 90 °C is spontaneously dissolved in water in both the presence and absence of $HCl_{(aq.)}$. This led to the conclusion that the presence of $HCl_{(aq.)}$ as well as a high dissolution temperature enhances the solubilization of collagen and breaks the collagen into low molecular weight peptides. This happens *via* the enhanced ionization of $HCl_{(aq.)}$, which in turn hydrolyse the collagen into water-soluble peptides with ionized amino acid residues available to be hydrated by water. During the regeneration process, DESs are washed away, and the H-bonding can be partially restored between the amino acids of collagen chains. Nevertheless, the regenerated material does not have the same amount and location of H-bonds as the native collagen. This results in variations in the structure and properties of regenerated material in comparison to native collagen.

3.2.7. Recyclability of DESs. The recyclability of DESs and the regenerated material is checked to validate the concept of sustainability in the present work. The DESs were recovered from their solutions in ethanol after filtering the regenerated material. FTIR spectra of the recycled DESs and the regenerated materials after processing at different temperatures in the absence and presence of $HCl_{(aq.)}$ are shown in Fig. 6A and S12, ESI,† respectively. Fig. 6A shows the retention of the most noticeable bands of ChCl and LA in the case of recycled ChCl : LA (ChCl: $-OH_{(str.)}$ ~3400–3500 cm^{-1}, $C-H_{(str.)}$ ~2800 cm^{-1} of the tertiary amine group, $C-N_{(str.)}$ and $C-H_{(bending)}$ in the range of 1300–1000 cm^{-1}, and LA: $C{=}O_{(str.)}$ in the range of 1700–1725 cm^{-1}, and the $C-O_{(str.)}$ in the range of 1000–1300 cm^{-1}). Most of the significant bands ~3000–3500 cm^{-1} related to $-OH_{(str.)}$ and bands ~2800–2950 cm^{-1} corresponding to $C-H_{(sym.)}$ and $C-H_{(asym.)}$ methylene group stretching are also retained upon recycling EG : $ZnCl_2$ DES.

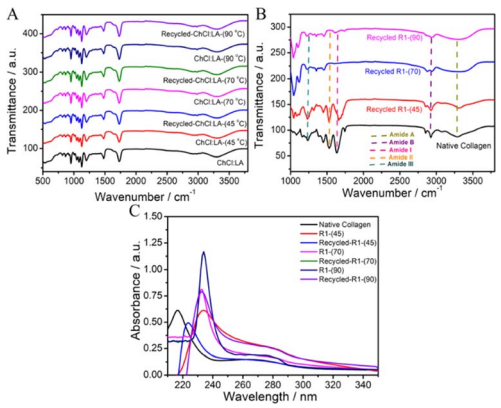

Fig. 6 (A) FTIR spectra of recycled ChCl : LA at different temperatures in comparison to native DES; (B) FTIR spectra of the material regenerated from the recycled ChCl : LA DES at different temperatures in comparison to native collagen; and (C) UV-vis spectra of material regenerated from recycled ChCl : LA DES at different temperatures in comparison to native collagen.

Further, the material regenerated after dissolution of collagen in recycled DESs displays bands similar to those observed in the case of materials regenerated from virgin DESs (Fig. 6B and S13, ESI†). A similar shift in amide bands in comparison to native collagen is observed in samples obtained from recycled DESs. Furthermore, the UV-vis absorbance spectra of regenerated material from recycled DESs (Fig. 6C) are observed to have similar bands at ~210–230 nm and ~270–300 nm as those observed for the material regenerated from the original DESs. A similar trend is observed in recycled DESs in the presence of $HCl_{(aq.)}$ (Fig. S14, ESI†). A comparable bathochromic and hyperchromic shift is also observed. This demonstrates the recyclable nature of DESs, which contributes to the sustainability of the dissolution process.

3.2.8. Antibacterial activity of regenerated material. The antibacterial activity of native and different regenerated collagen samples at 0.5 mg ml^{-1} was evaluated against different bacterial strains (Table 2). All the regenerated samples showed significantly higher bacterial growth inhibition compared to native collagen and comparable to or greater than that exhibited by Kanamycin in many cases. Collagen peptides are well known for their antimicrobial activity, which is regulated by many factors, including their size, sequence, and charge.[70] The antimicrobial activity of R1-(45)-A and R2-(45)-A is similar to that of Kanamycin against Gram-negative bacteria. Similarly, water insoluble and soluble R1-(70)-A and R2-(70)-A possess antimicrobial activity equivalent to that of Kanamycin against both Gram-positive and Gram-negative bacteria. A similar observation is obtained for collagen peptides R1-(90), R1-(90)-A and R2-(90) except for R2-(90)-A against *Escherichia coli* bacteria. The formation of collagen peptides is accompanied by the induction of a positive charge *via* the breakage of ionic bonds as well as the interaction of excess H^+ with imino groups of proline and hydroxyproline, resulting in the formation of ammonium salt.

Such positively charged peptides undergo electrostatic interactions with the negatively charged bacterial membranes.[13,50] Following this, the aromatic amino acid residues of collagen and collagen peptides are exposed towards solvent upon unfolding during dissolution, especially at high temperatures, and the presence of $HCl_{(aq.)}$ facilitates the anchoring of such hydrophobic amino acid residues to the hydrophobic lipid core of the bacterial membrane.[71] According to the barrel-stave model, small cationic peptides adsorb on the surface of bacteria and their hydrophobic amino acid groups are embedded into the membrane, resulting in the formation of pores.[72]

These pores block bacterial functioning by interacting with their DNAs and RNAs. Further, the efficient antimicrobial activity shown by water soluble R1-(70)-A and R2-(70)-A compared to that of R1-(90), R2-(90), R1-(90)-A and R2-(90)-A can

Table 2 Antibacterial activity (% growth inhibition) of native and regenerated collagen samples with 0.5 mg ml^{-1} concentration against different bacterial strains[a]

Sample	*Escherichia coli*	*Pseudomonas syringae*	*Bacillus subtilis*	*Staphylococcus aureus*
Buffer	2.69 ± 0.13^{g}	10.41 ± 0.54^{i}	6.16 ± 0.28^{j}	4.88 ± 0.62^{n}
Kanamycin	86.02 ± 1.30^{a}	90.58 ± 1.73^{a}	83.21 ± 0.56^{b}	91.95 ± 0.26^{a}
Native	40.30 ± 0.39^{f}	12.54 ± 0.42^{h}	27.95 ± 1.03^{i}	13.53 ± 0.92^{m}
R1-(45)	73.41 ± 0.79^{d}	81.80 ± 0.36^{c}	71.27 ± 0.58^{f}	85.39 ± 0.83^{c}
R2-(45)	77.33 ± 1.12^{b}	81.12 ± 0.28^{c}	62.61 ± 0.21^{h}	87.35 ± 0.37^{b}
R1-(45)-A	75.44 ± 1.13^{c}	86.46 ± 0.32^{b}	77.17 ± 0.53^{d}	54.33 ± 1.31^{l}
R2-(45)-A	85.86 ± 1.41^{a}	59.23 ± 0.28^{f}	80.03 ± 0.59^{c}	76.70 ± 1.60^{g}
R1-(70)	73.52 ± 1.29^{d}	70.09 ± 0.34^{e}	74.88 ± 0.39^{e}	66.42 ± 0.94^{i}
R2-(70)	66.98 ± 1.37^{e}	80.09 ± 0.37^{c}	62.57 ± 0.20^{h}	56.14 ± 0.52^{k}
R1-(70)-A-water insoluble	86.66 ± 1.30^{a}	82.89 ± 0.46^{c}	65.50 ± 0.50^{g}	77.22 ± 0.67^{f}
R2-(70)-A-water insoluble	86.75 ± 0.92^{a}	87.51 ± 0.46^{b}	87.76 ± 0.47^{a}	91.86 ± 0.58^{a}
R1-(70)-A-water soluble	85.94 ± 1.39^{a}	86.18 ± 0.45^{b}	82.60 ± 0.38^{b}	80.84 ± 0.65^{e}
R2-(70)-A-water soluble	86.82 ± 1.45^{a}	86.85 ± 0.61^{b}	65.66 ± 0.27^{g}	78.15 ± 0.44^{f}
R1-(90)	75.26 ± 1.83^{c}	71.67 ± 0.73^{e}	75.32 ± 0.39^{e}	69.27 ± 0.33^{h}
R1-(90)	76.81 ± 1.82^{c}	50.43 ± 0.74^{g}	78.60 ± 0.39^{d}	59.58 ± 0.94^{j}
R1-(90)-A	85.79 ± 1.38^{a}	76.97 ± 1.03^{d}	76.23 ± 0.51^{e}	82.00 ± 0.13^{d}
R2-(90)-A	78.42 ± 1.07^{b}	86.67 ± 0.84^{b}	85.31 ± 0.90^{a}	86.88 ± 0.42^{b}

[a] Data represent the mean ± SE of three independent biological replicates. Different letters (a–n) within the column represent values that were significantly different among different samples (Fisher LSD; $p \leq 0.05$).

correlate with the decreasing number of peptides in the given fraction with an increase in temperature as evidenced by SDS PAGE as a higher number of collagen peptides are considered to exhibit better antimicrobial properties.[13]

4 Conclusions

A simple, sustainable, and robust method for the dissolution and regeneration of type I collagen in DESs, along with its transformation to water soluble collagen peptides, is established. DESs, *i.e.* ChCl : LA (1 : 1) and EG : $ZnCl_2$ (4 : 1), have shown remarkable dissolving ability towards collagen, which increases with an increase in the temperature of dissolution. EG : $ZnCl_2$ is more effective in dissolving collagen than ChCl : LA at any investigated temperature. The presence of $[HCl_{(aq.)}] = 5 \times 10^{-5}$ M increases the solubility of collagen by 2–5 w/v% depending on the nature of DES and temperature although no change in pH occurs. Collagen is dissolved in DESs following alterations in the 2°-structure, where a higher dissolution temperature and the presence of H^+ result in greater unwinding of the triple-helical structure of collagen. Alterations in the 2°-structure accompanied by cleavage of peptide bonds lead to the formation of low molecular weight collagen peptides that are readily soluble in water. The regenerated material shows good antimicrobial activity towards both Gram-positive and Gram-negative bacteria, which is even more than that shown by the standard antibiotic Kanamycin, especially in the case of collagen peptides. After regeneration of the dissolved collagen, the recovered DESs show no structural alterations compared to native DESs and are reused for the dissolution of collagen. Along with the previous studies on the extraction of collagen using DESs,[39,40] the present work would pave a platform for the dissolution and stabilization of other biologically important polymers in DESs with new implications for human health and food safety.

Data availability

The data will be made available on request.

Author contributions

Harmandeep Kaur (experimentation, data analysis and drafting of manuscript); Navdeep Kaur (antimicrobial activity and concerned data analysis); Pratap Kumar Pati (data analysis, supervision); Monika Rani (SDS-PAGE); Tejwant Singh Kang (conceptualization, supervision, data analysis and manuscript writing). All authors have given approval to the final version of the manuscript.

Conflicts of interest

There are no conflicts to declare.

Acknowledgements

This work was supported by CSIR, Govt of India wide project number 01(3018)/21/ EMR-II and DST-SERB (CRG/2021/005897). The infrastructure provided for this work under the UPE grant and UGC-CAS (Centre for Advanced Studies) program is highly acknowledged. H. K. is thankful to CSIR, Govt of India, M. S. is thankful to UGC, Govt of India, N. K. is thankful to DST-Woman Scientist-A (WOS-A) for fellowship.

References

1 S. Noorzai, C. J. R. Verbeek, M. C. Lay and J. Swan, *Waste Biomass Valorization*, 2020, **11**, 5687–5698.

2 A. León-López, A. Morales-Peñaloza, V. M. Martínez-Juárez, A. Vargas-Torres, D. I. Zeugolis and G. Aguirre-Álvarez, *Molecules*, 2019, **24**, 4031–4047.
3 S. W. Chang, S. J. Shefelbine and M. J. Buehler, *Biophys. J.*, 2012, **102**(3), 640–648.
4 J. Lei, B. Zou, R. Zhang, K. Zhang, R. Xie, W. Zhang, J. Wu, S. Li, B. Zheng and F. Huo, *J. Leather Sci. Eng.*, 2019, **1**(1), 1–9.
5 N. O. Metreveli, K. K. Jariashvili, L. O. Namicheishvili, D. V. Svintradze, E. N. Chikvaidze, A. Sionkowska and J. Skopinska, *Ecotoxicol. Environ. Saf.*, 2010, **73**, 448–455.
6 G. C. Na, *Top. Catal.*, 1988, **8**, 315–330.
7 T. Miyahara, A. Murai, T. Tanaka, S. Shiozawa and M. Kameyama, *J. Gerontol.*, 1982, **37**, 651–655.
8 M. D. Shoulders and R. T. Raines, *Annu. Rev. Biochem.*, 2009, **78**, 929–958.
9 N. Rajan, J. Habermehl, M. F. Coté, C. J. Doillon and D. Mantovani, *Nat. Protoc.*, 2007, **1**, 2753–2758.
10 P. Mokrejs, F. Langmaier, M. Mladek, D. Janacova, K. Kolomaznik and V. Vasek, *Waste Manage. Res.*, 2009, **27**, 31–37.
11 D. Liu, M. Nikoo, G. Boran, P. Zhou and J. M. Regenstein, *Annu. Rev. Food Sci. Technol.*, 2015, **6**, 527–557.
12 G. Singh, G. Singh, K. Damarla, P. K. Sharma, A. Kumar and T. S. Kang, *ACS Sustain. Chem. Eng.*, 2017, **5**, 6568–6577.
13 M. C. Gomez-Guillen, B. Gimenez, M. E. Lopez-Caballero and M. P. Montero, *Food Hydrocolloids*, 2011, **25**, 1813–1827.
14 J. Ao and B. Li, *Food Sci. Technol. Int.*, 2012, **18**, 425–434.
15 D. Dumitriu and T. Dobre, *J. Endod.*, 2015, **41**, 903–906.
16 P. Qi, Y. Zhou, D. Wang, Z. He and Z. Li, *RSC Adv.*, 2015, **5**, 87180–87186.
17 K. Jariashvili, B. Madhan, B. Brodsky, A. Kuchava, L. Namicheishvili and N. Metreveli, *Biopolymers*, 2012, **97**, 189–198.
18 Y. Hu, L. Liu, W. Dan, N. Dan and Z. Gu, *J. Appl. Polym. Sci.*, 2013, **130**, 2245–2256.
19 Z. Meng, X. Zheng, K. Tang, J. Liu, Z. Ma and Q. Zhao, *Int. J. Biol. Macromol.*, 2012, **51**, 440–448.
20 Z. Lei, B. Chen, Y. M. Koo and D. R. Macfarlane, *Chem. Rev.*, 2017, **117**, 6633–6635.
21 C. Mukesh, D. Mondal, M. Sharma and K. Prasad, *Chem. Commun.*, 2013, **49**, 6849–6851.
22 J. S. Wilkes, *Green Chem.*, 2002, **4**, 73–80.
23 A. Tarannum, A. Adams, B. Blümich and N. N. Fathima, *J. Phys. Chem. B*, 2018, **122**, 1060–1065.
24 A. Tarannum, R. R. Jonnalagadda and N. F. Nishter, *Spectrochim. Acta, Part A*, 2019, **212**, 343–348.
25 H. Zhang, J. Wu, J. Zhang and J. He, *Macromolecules*, 2005, **38**, 8272–8277.
26 K. Singh, S. Mehra and A. Kumar, *Green Chem.*, 2022, **24**, 9629–9642.
27 S. Liu, Q. Li and G. Li, *J. Leather Sci. Eng.*, 2019, **1**, 1–12.
28 B. Soares, A. M. da Costa Lopes, A. J. Silvestre, P. C. R. Pinto, C. S. Freire and J. A. Coutinho, *Ind. Crops Prod.*, 2021, **160**, 113128.
29 H. Garcia, R. Ferreira, M. Petkovic, J. L. Ferguson, M. C. Leitão, H. N. Gunaratne, R. Seddonab Kenneth, N. Rebelo Luís Paulo and C. S. Pereira, *Green Chem.*, 2010, **12**(3), 367–369.
30 A. Idris, R. Vijayaraghavan, U. A. Rana, A. F. Patti and D. R. Macfarlane, *Green Chem.*, 2014, **16**, 2857–2864.
31 D. M. Phillips, L. F. Drummy, D. G. Conrady, D. M. Fox, R. R. Naik, M. O. Stone, P. C. Trulove, H. C. De Long and R. A. Mantz, *J. Am. Chem. Soc.*, 2004, **126**, 14350–14351.
32 E. L. Smith, A. P. Abbott and K. S. Ryder, *Chem. Rev.*, 2014, **114**, 11060–11082.
33 A. Abo-Hamad, M. Hayyan, M. A. H. AlSaadi and M. A. Hashim, *J. Chem. Eng.*, 2015, **273**, 551–567.
34 Y. Dai, J. van Spronsen, G. J. Witkamp, R. Verpoorte and Y. H. Choi, *Anal. Chim. Acta*, 2013, **766**, 61–68.
35 D. Carriazo, M. C. Serrano, M. C. Gutiérrez, M. L. Ferrer and F. del Monte, *Chem. Soc. Rev.*, 2012, **41**, 4996–5014.
36 A. S. Khan, T. H. Ibrahim, N. A. Jabbar, M. I. Khamis, P. Nancarrow and F. S. Mjalli, *RSC Adv.*, 2021, **11**, 12398–12422.
37 E. M. Nuutinen, P. Willberg-Keyriläinen, T. Virtanen, A. Mija, L. Kuutti, R. Lantto and A. S. Jääskeläinen, *RSC Adv.*, 2019, **9**, 19720–19728.
38 D. Wang, X. H. Yang, R. C. Tang and F. Yao, *Polymers*, 2018, **10**(9), 993.
39 C. Bai, Q. Wei and X. Ren, *ACS Sustain. Chem. Eng.*, 2017, **5**, 7220–7227.
40 M. Bisht, M. Martins, A. C. R. V. Dias, S. P. M. Ventura and J. A. P. Coutinho, *Green Chem.*, 2021, **23**, 8940–8948.
41 H. Zhang, J. Lang, P. Lan, H. Yang, J. Lu and Z. Wang, *Mater. Polym.*, 2018, **10**(9), 993.
42 Q. Wang, X. Yao, Y. Geng, Q. Zhou, X. Lu and S. Zhang, *Green Chem.*, 2015, **17**, 2473–2479.
43 L. Zhou, X. Lu, Z. Ju, B. Liu, H. Yao, J. Xu, Q. Zhou, Y. Hu and S. Zhang, *Green Chem.*, 2019, **21**, 897–906.
44 H. Kaur, M. Singh, H. Singh, M. Kaur, G. Singh, K. Sekar and T. S. Kang, *Green Chem.*, 2022, **24**, 2953–2961.
45 H. Kaur, M. Singh, K. Singh, A. Kumar and T. S. Kang, *Green Chem.*, 2023, **25**, 5172–5181.
46 X. Tan, Y. Wang, W. Du and T. Mu, *ChemSusChem*, 2020, **13**, 321–327.
47 X. Tan, W. Zhao and T. Mu, *Green Chem.*, 2018, **20**, 3625–3633.
48 P. Kalhor, K. Ghandi, H. Ashraf and Z. Yu, *Phys. Chem. Chem. Phys.*, 2021, **23**, 13136–13147.
49 R. Alcalde, A. Gutiérrez, M. Atilhan and S. Aparicio, *J. Mol. Liq.*, 2019, **290**, 110916.
50 N. Ennaas, R. Hammami, A. Gomaa, F. Bédard, É. Biron, M. Subirade, L. Beaulieu and I. Fliss, *Biochem. Biophys. Res. Commun.*, 2016, **473**, 642–647.
51 B. De Campos Vidal and M. L. S. Mello, *Micron*, 2011, **42**, 283–289.
52 M. G. Bridelli, in *Fourier Transforms – HigH-Tech Application and Current Trends*, InTech, 2017.
53 S. Y. Bak, S. W. Lee, C. H. Choi and H. W. Kim, *Materials*, 2018, **11**(12), 2518.
54 M. Vedhanayagam, S. Anandasadagopan, B. U. Nair and K. J. Sreeram, *Mater. Sci. Eng., C*, 2020, **108**, 110378.
55 K. J. Payne and A. Veis, *Biopolymers*, 1988, **27**(11), 1749–1760.

56 V. Gauba and J. D. Hartgerink, *J. Am. Chem. Soc.*, 2007, **129**, 2683–2690.
57 N. J. Greenfield, *Nat. Protoc.*, 2006, **1**(6), 2876–2890.
58 R. W. Woody, *J. Am. Chem. Soc.*, 2009, **131**, 8234–8245.
59 N. T. Chinh, V. Q. Manh, V. Q. Trung, T. D. Lam, M. D. Huynh, N. Q. Tung, N. D. Trinh and T. Hoang, *Nat. Prod. Commun.*, 2019, **14**(7), 7–19.
60 F. Zsila, *Anal. Biochem.*, 2022, **639**, 114512.
61 Q. Y. Han, T. Koyama, S. Watabe, Y. Nagashima and S. Ishizaki, *Molecules*, 2023, **28**(2), 889.
62 D. Li, C. Mu, S. Cai and W. Lin, *Ultrason. Sonochem.*, 2009, **16**, 605–609.
63 F. Zhang, A. Wang, Z. Li, S. He and L. Shao, *Food Nutr. Sci.*, 2011, **02**, 818–823.
64 M. Ahmad, N. P. Nirmal and J. Chuprom, *RSC Adv.*, 2016, **6**, 33868–33879.
65 A. Sionkowska, J. Skopinska-Wisniewska, M. Gawron, J. Kozlowska and A. Planecka, *Int. J. Biol. Macromol.*, 2010, **47**, 570–577.
66 D. Kathyayani, B. Mahesh, N. A. Chamaraja, B. S. Madhukar and D. C. Gowda, *Colloids Surf., A*, 2022, **649**, 129503.
67 C. Hermida-Merino, D. Cabaleiro, C. Gracia-Fernández, J. Valcarcel, J. A. Vázquez, N. Sanz, M. Pérez-Rodríguez, M. Arenas-Moreira, D. Banerjee, A. Longo, C. Moya-Lopez, L. Lugo, P. Bourson, A. B. Pereiro, G. Salloum-Abou-Jaoude, I. Bravo, M. M. Piñeiro and D. Hermida-Merino, *Gels*, 2022, **8**(9), 594.
68 O. S. Rabotyagova, P. Cebe and D. L. Kaplan, *Mater. Sci. Eng., C*, 2008, **28**(8), 1420–1429.
69 J. Wu, Z. Li, X. Yuan, P. Wang, Y. Liu and H. Wang, *Trans. Tianjin Univ.*, 2011, **17**, 111–117.
70 G.-G. Mc, L.-C. Me, A. A. López, L. A. Giménez and B. Montero, *Sea By-Products as a Real Material: New Ways of Application*, 2010, vol. 37, pp. 89–115.
71 N. Ennaas, R. Hammami, L. Beaulieu and I. Fliss, *Biochem. Biophys. Res. Commun.*, 2015, **462**, 195–200.
72 J. Lei, L. Sun, S. Huang, C. Zhu, P. Li, J. He, V. Mackey, D. H. Coy and Q. He, *Am. J. Transl. Res.*, 2019, **11**(7), 3919.